Supporting information for

Ti-mesh supported porous CoS2 nanosheets self-interconnecting net-work with high oxidation states for efficient hydrogen production via urea electrolysis

Yu Jiang,[†] ShanShan Gao,[,†,‡,§] JinLing Liu,[†] GongChen Xu,[†] Jia Qiang, [†] FuShan Chen,[†] and XiaoMing Song[*,†]*

[†]Qingdao University of Science and Technology, 53 Zhengzhou Road, 266042, Qingdao, P. R. China.

[‡]Guangxi University, Nanning 530004, P. R. China.

[§]Qilu University of Technology, Jinan 250353, Shandong Province, P. R. China

[*]E-mail address: jyu4341@163.com; xiaomingsong4007@163.com

Experimental section

Reagents. Cobalt (II) nitrate hexahydrate ($Co(NO_3)_2$ $6H_2O$), Aluminum nitrate nonahydrate ($Al(NO_3)_3$ $9H_2O$), Urea (CH_4N_2O), Ammonium fluoride (NH_4F), Sodium hydroxide (NaOH), Potassium hydroxide (KOH), Ethanol absolute were supplied from Sinopharm Chemical Reagent Co. Ltd (www.sinoreagent.com). Sulfur sublimed (AR) was obtained from Tianjin Damao Chemical Reagent Factory. Pt/C (20%) and RuO_2 (99.9%) were purchased from Shanghai Macklin Biochemical Co., Ltd (Shanghai, China).

Synthesis of CCH&Al(OH)$_3$/Ti. The precursor of CCH&$Al(OH)_3$/Ti was prepared using a facile vapor-phase hydrothermal method. In this process, 1.7462 g $Co(NO_3)_2$ $6H_2O$, 0.2251 g $Al(NO_3)_3$ $6H_2O$, 1.2012 g Urea, 0.1482 g NH_4F and 40 mL ultra-pure water were mixed thoroughly to provide a homogeneous solution, and then immediately added into 50 mL Teflonlined autoclave. Next, we put the cleaned Ti mesh against the wall of Teflon-liner and heated at 110 ℃ for 8 h, and then naturally cooled it to room temperature. The acquired sample was cleaned with deionized water and ethanol enough with the assistance of ultrasonic and dried it at 60 ℃.

Synthesis of Co(OH)$_2$&Co+3O(OH)/Ti. The process was selectively etching amphoteric Al in CCH&$Al(OH)_3$/Ti. As prepared precursor was transferred to 3.0 M NaOH against the wall of Erlenmeyer flask for 10 hours. Then the acquired $Co(OH)_2$&Co+3O(OH)/Ti was cleaned with deionized water and ethanol enough and then dried it at room temperature.

Synthesis of P-CoS_2/Ti. The step was acquired P-CoS_2/Ti by Chemical Vapor Deposition with 1.0 g sulfur powder. The as-synthesized $Co(OH)_2$&Co+3O(OH)/Ti and 1.0 g sulfur powder were placed in two porcelain boat separately, and 1.0 g sulfur powder was at the upstream side of the tube furnace. The samples were calcined at 300 °C for 2 h with a heating rate of 5 °C min^{-1} in N_2 flow, and then naturally cooled to ambient temperature. Composites with different temperatures (400 °C, 500 °C and 600 °C) for chemical vapor deposition were synthesized using the same procedure for comparison. The effect of etching with different alkali concentrations on the catalytic performance was also studied.

Synthesis of CoS_2/Ti. For comparison, the CoS_2 on the Ti mesh was synthesized as reference.[1] 1.7462 g $Co(NO_3)_2$ $6H_2O$, 1.2012 g urea, 0.1482 g NH_4F and 40 mL ultra-pure water were mixed thoroughly to provide a homogeneous solution. Then we put the solution and one piece of cleaned Ti mesh into 50 mL Teflonlined autoclave. The autoclave was then tightly sealed and left in an oven at 110 °C for 8 h for reaction. The acquired sample and 1.0 g sulfur powder were placed in two porcelain boat separately, and 1.0 g sulfur powder was at the upstream side of the tube furnace. The samples were calcined at 300 °C for 2 h with a heating rate of 5 °C min^{-1} in N_2 flow, and then naturally cooled to ambient temperature.

Synthesis of Pt/C and RuO_2 electrodes. For comparison, to synthesize the Pt/C and RuO_2 electrodes (3.1 mg cm^{-2}) as follows: 10 mg Pt/C (20 wt %) or 99.9 % RuO_2 was well dispersed in 0.9 mL of 4:1 (v/v) water/ethanol and 0.1 mL 0.5% wt Nafion

solution by sonication for 30 min to form a homogeneous suspension. Then 155 uL homogeneous suspension was drop cast onto bare Ti mesh (1×0.5 cm^2) and dried it at room temperature.

Electrochemical measurements. The electrochemical measurements of the samples were conducted using CHI-760E electrochemical workstation at room temperature. The HER and UOR catalytic activities were tested by using a three-electrode system in a 1.0 M KOH with 0.3 M urea (PH=14). Using a graphite rod and an Hg/HgO electrode as the counter electrode and reference electrode, respectively. The prepared samples (0.5×0.5 cm^2) were adopted as the working electrode. The loadings of CCH&$Al(OH)_3$/Ti, $Co(OH)_2$&Co+3O(OH)/Ti, CoS_2/Ti and P-CoS_2/Ti are 2.95, 2.35, 3.88 and 3.1 mg cm^{-2}. Polarization curves were obtained at a scan rate of 5 mV s^{-1}. All the measured potentials were calibrated to the reversible hydrogen electrode (RHE) using the following equation: $E_{RHE} = E_{Hg/HgO} + 0.098 + 0.059$ PH. The polarization curves were corrected using the equation: $E_{compensated} = E_{measured} - iR_s$ (R_s is the series resistance determined by EIS). The percentage of iR corrected in the electrochemical analysis is 80%. The Tafel plots was obtained from LSV curves using the Tafel equation: $\eta = b \log j + a$ (j is the current density, b is the Tafel slope). For overall water splitting, using P-CoS_2/Ti as both the cathode and the anode in a two-electrode system. Cyclic voltammograms (CV) were recorded in 1.0 M KOH and 0.3 M urea with different scan rates from 10 to 50 mV s^{-1} in the potential range of 0.7-0.8 V (vs.RHE). EIS measurements were conducted with a scan rate of 5 mV s^{-1}. The frequency ranges from 1000000 to 0.01 Hz.

Physical Methods. X-ray diffraction (XRD, BRUKER D8 ADVANCE) was used to certify the crystal structures of as-prepared samples. Scanning electron microscope (SEM) and energy dispersive X-ray analyzer (EDX) were conducted using an JSM-6700. The TEM images and HRTEM images were recorded using a JEM 2100 Plus operated at 200 kV. The surface chemical composition and valence of the samples were analyzed with X-ray photoelectron spectra (XPS, Thermo fisher ESCALAB 250 X-ray photoelectron spectrometer). The specific surface area and pore size distribution of the catalyst were measured by using an ASAP2020 at 77 K. The Raman spectra of the prepared samples were measured by using a Renishaw Invia Reflex Raman system with 532 nm diode laser excitation.

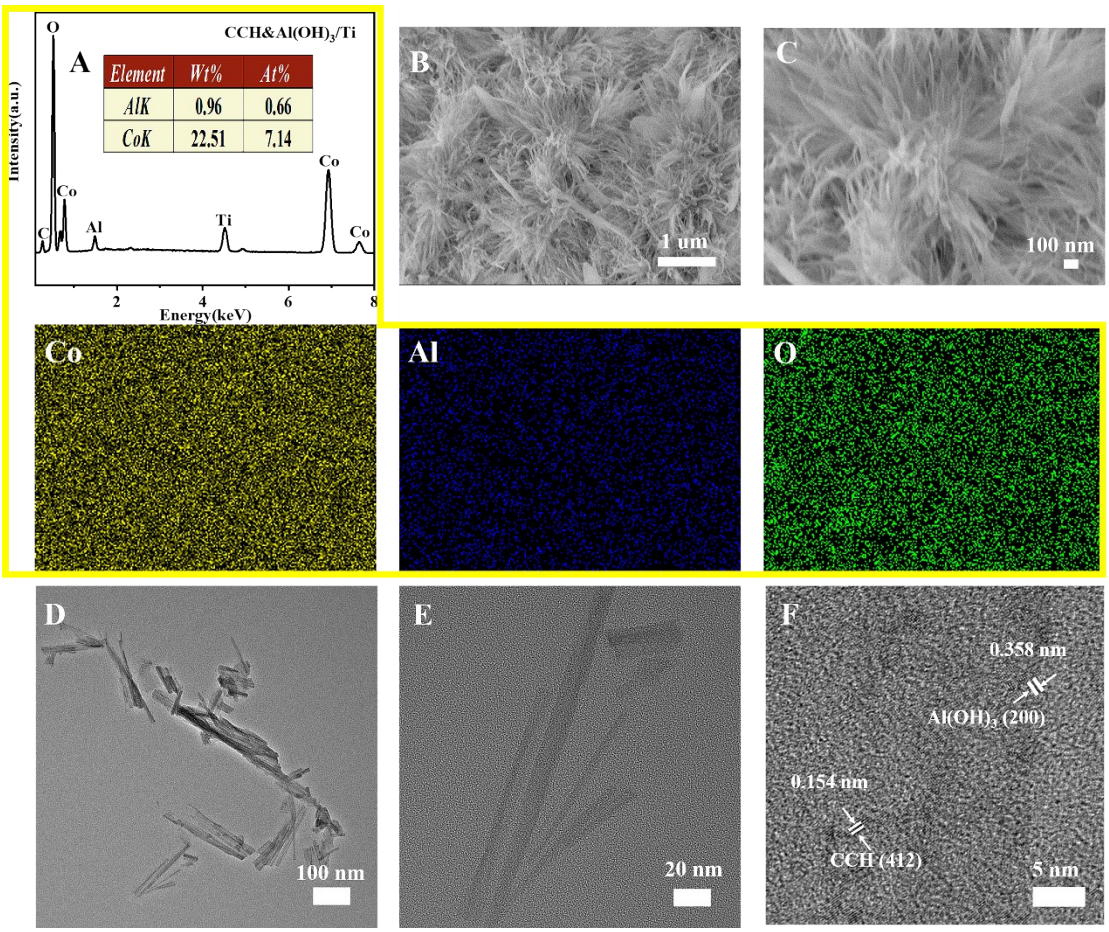

Figure S1. Characterization of CCH&Al(OH)$_3$/Ti. EDX spectrum and elemental mapping (Co, Al and O) (A). SEM images at different magnifications (B, C). TEM images at different magnifications (D, E). HRTEM image (F).

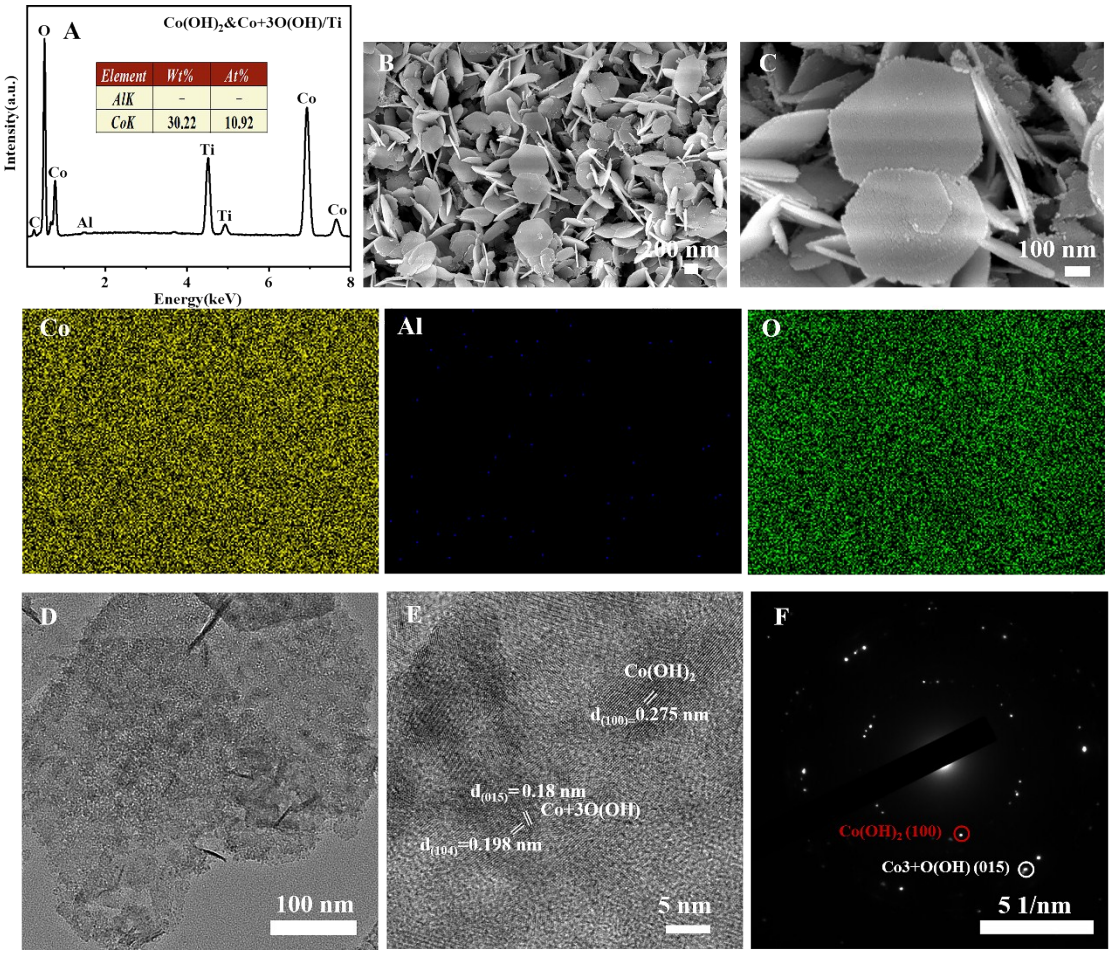

Figure S2. Characterization of $Co(OH)_2$&Co+3O(OH)/Ti. (A) EDX specture and elemental mapping (Co, Al and O). SEM image (B, C). TEM image (D). HRTEM image (E). SAED pattern (F).

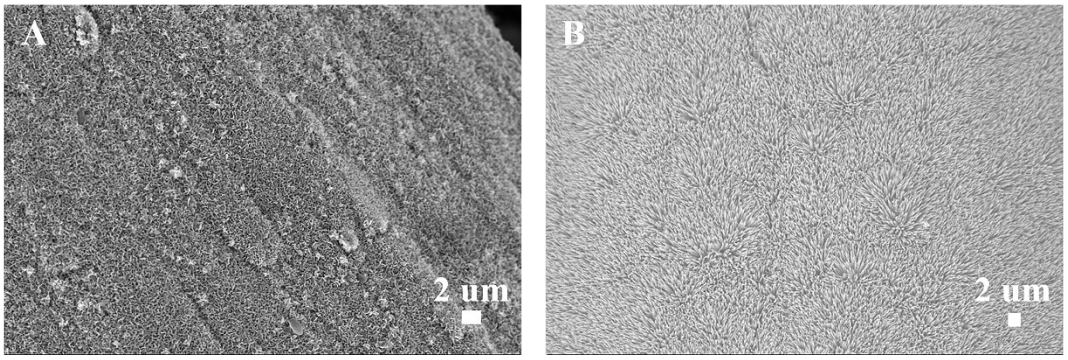

Figure S3. (A) The low magnification SEM image of P-CoS_2/Ti, (B) The low magnification SEM image of CoS_2/Ti.

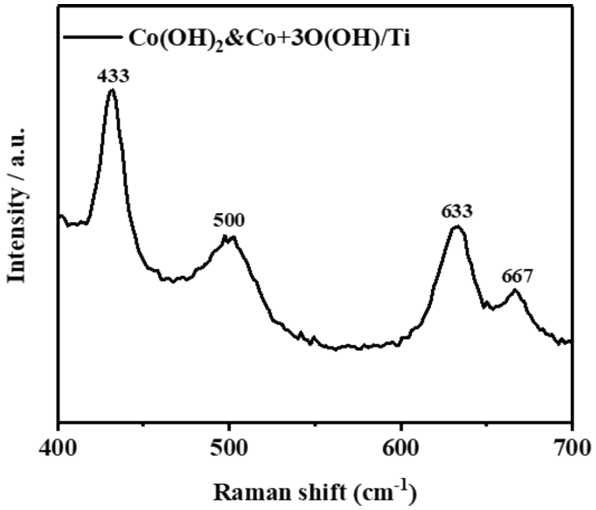

Figure S4. Raman spectrum of $Co(OH)_2$&Co+3OOH/Ti.

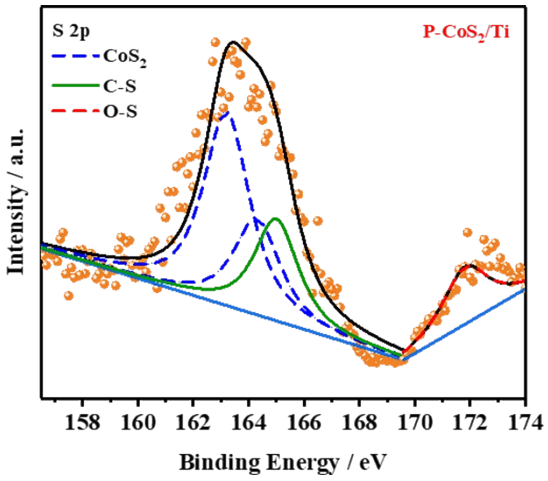

Figure S5. The S 2p XPS spectra for P-CoS_2/Ti

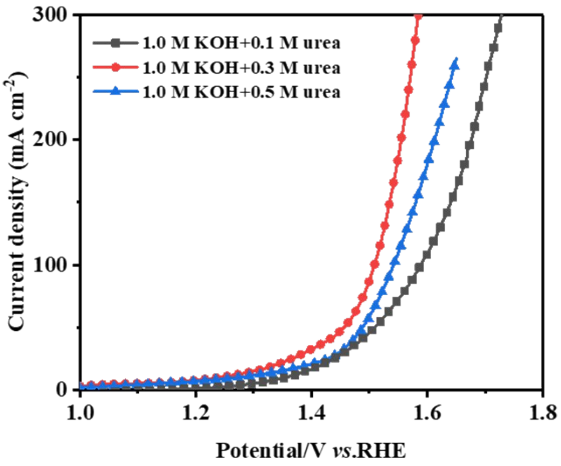

Figure S6. LSV curves of P-CoS_2/Ti in 1.0 M KOH with 0.1 M, 0.3 M and 0.5 M urea, respectively.

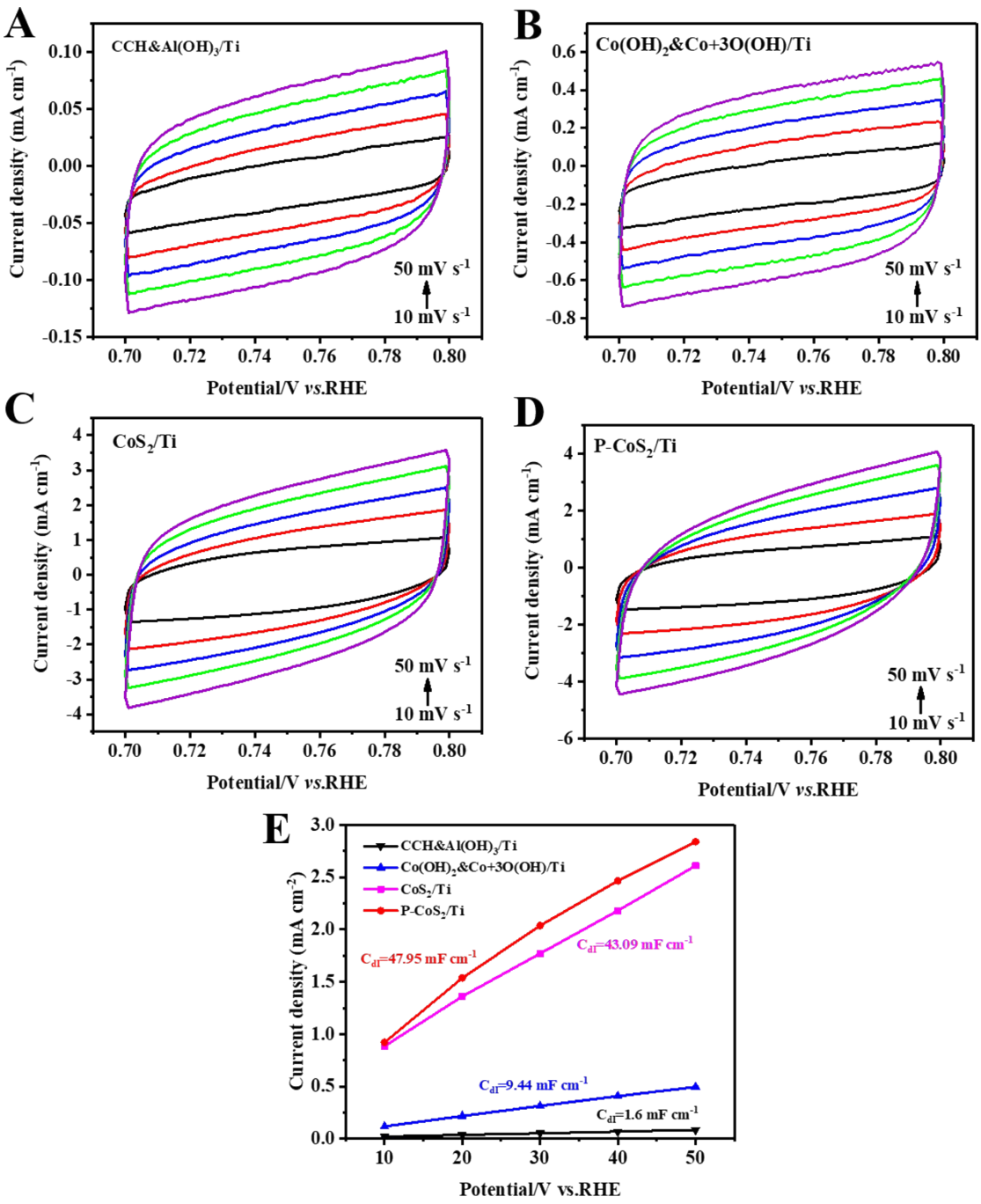

Figure S7. Cyclic voltammetry curves of CCH&Al(OH)$_3$/Ti (A), Co(OH)$_2$&Co+3O(OH)/Ti (B), CoS_2/Ti (C) and P-CoS_2/Ti (D). Estimation of C_{dl} by plotting the current density variation $\Delta j = (j_a - j_c)/2$ at 0.75 V (vs.RHE) vs scan rates (E).

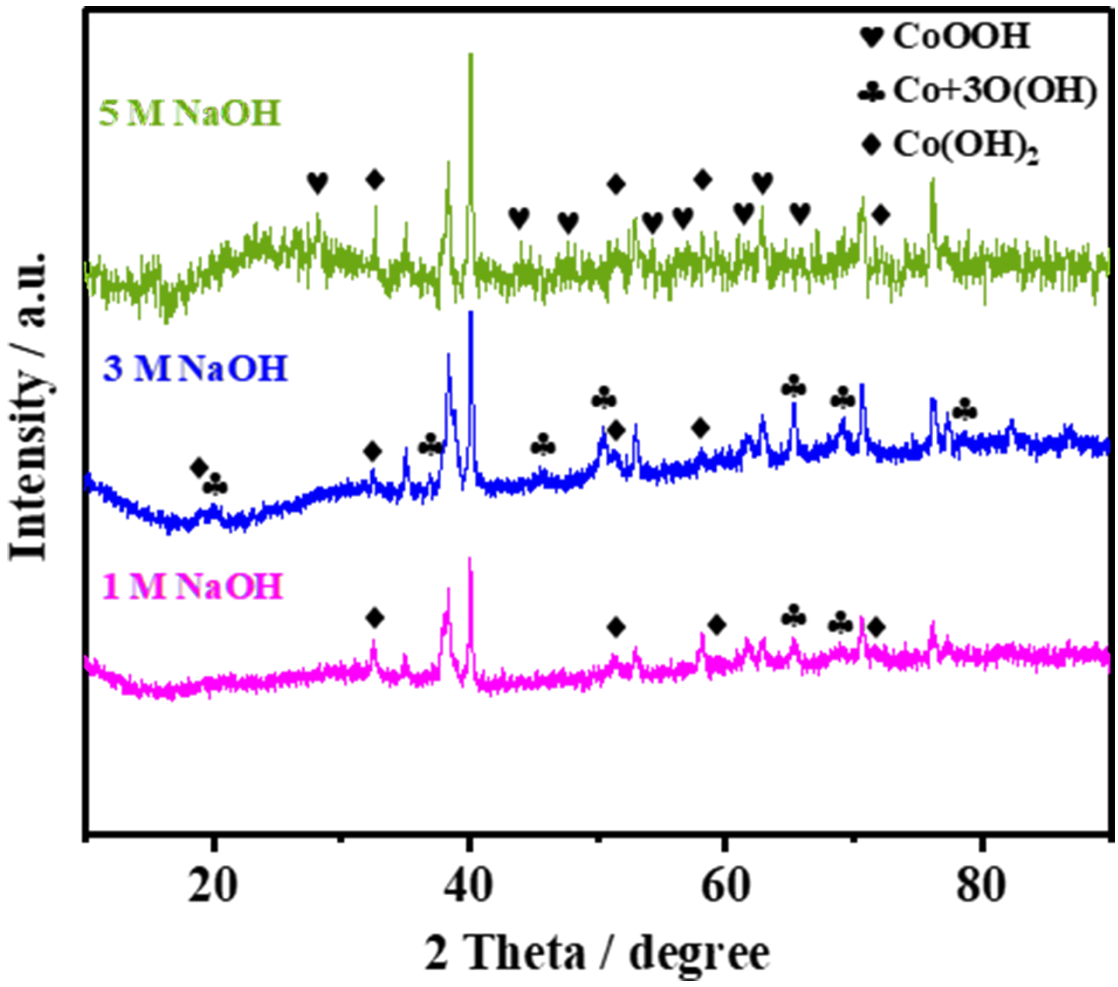

Figure S8. XRD pattern of $Co(OH)_2$&Co+3O(OH)/Ti prepared with different concentrations (1 M, 3 M and 5 M) of NaOH.

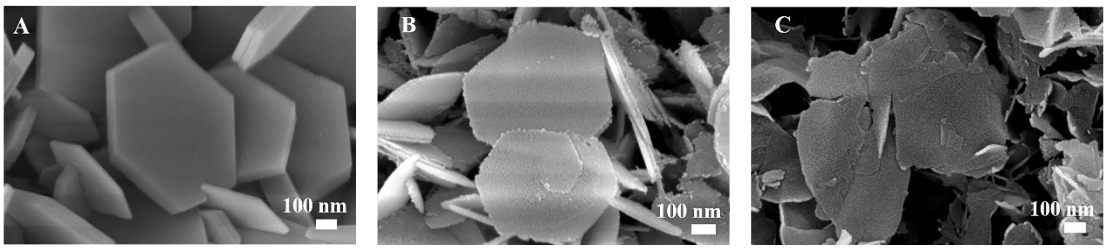

Figure S9. The SEM images of $Co(OH)_2$&Co+3O(OH)/Ti prepared with different concentrations of NaOH, (A) 1.0 M NaOH, (B) 3.0 M NaOH and (C) 5.0 M NaOH.

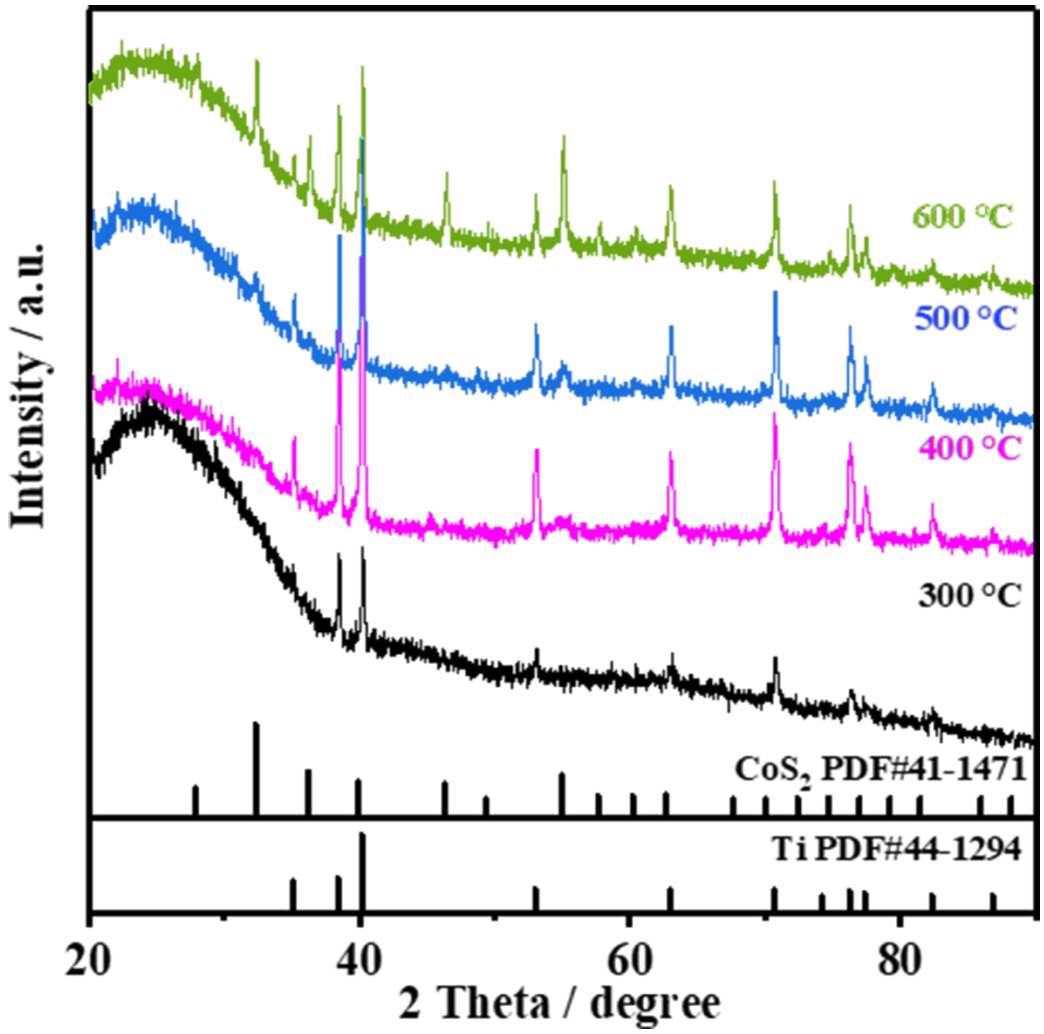

Figure S10. XRD pattern of P-CoS_2/Ti prepared at different calcination temperature for 2 h under N_2 atmosphere.

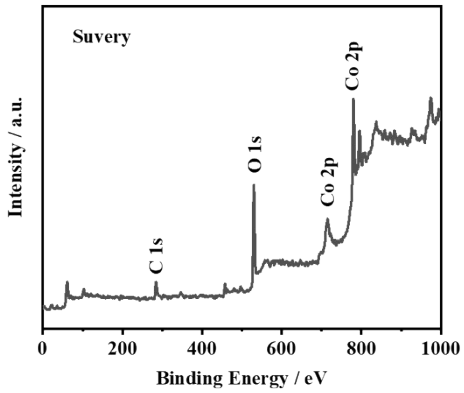

Figure S11. XPS survey spectrum of P-CoS_2/Ti after UOR: survey scan.

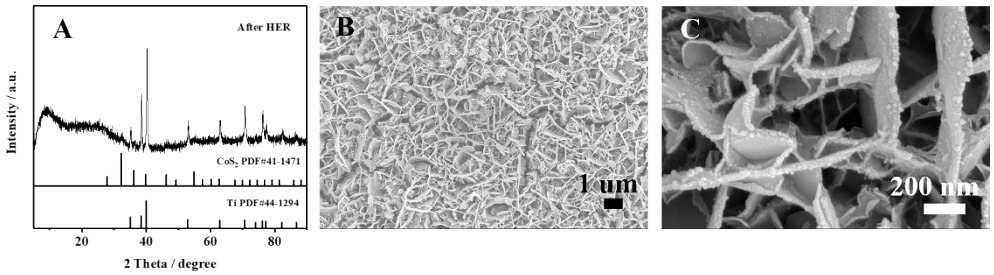

Figure S12. Characterization of P-CoS_2/Ti after the long-term stability test for HER. (A) XRD pattern, (B) low magnification SEM image, (C) high magnification SEM image.

Table S1. The information (Position, FWHM and Areas) on XPS fitting.

P-CoS_2/Ti (Co 2p)	FWHM	Areas
778.6 eV	2	4.5
782.3 eV	2	2
786.2 eV	3.5	9.5
790 eV	3	4
793.6 eV	2	2.3
798.3 eV	2	1
802	3.5	4
806.4	3	2

P-CoS_2/Ti (O 1s)	FWHM	Areas
530 eV	0.94	3
531.6 eV	1.3	4.5
532.8 eV	1.1	3
535.4 eV	2.68	21

P-CoS_2/Ti (S 2p)	FWHM	Areas
163.2 eV	2	3.2
164.3 eV	2	1.6
165 eV	1.9	1.6
171.8 eV	1.98	0.9

CoS_2/Ti (Co 2p)	FWHM	Areas
775 eV	3.3	2.6
781.6 eV	6	10.4
786 eV	1.8	0.8
789.6 eV	3.3	1.3
797.6 eV	6	5.2
803 eV	1.7	0.5

CoS_2/Ti (O 1s)	FWHM	Areas
524.4 eV	1.62	3.3
529.9 eV	4	12
531.7 eV	1.96	9
532.6 eV	0.6	1

P-CoS_2/Ti after UOR (Co 2p)	FWHM	Areas
779.85 eV	2.3	25841
789.9 eV	2.37	1618

794.94 eV	2.28	10031
804.35 eV	3.97	2269.5

P-CoS_2/Ti after UOR (O 1s)	FWHM	Areas
529.8 eV	2.2	20000
531.3 eV	1.4	4500
532.4 eV	1	800

Table S2. Comparison of HER performance for P-CoS_2/Ti with other catalysts in 1.0 M KOH.

Electrocatalyst	Electrolyte solution	Overpotential at 10 mA cm^{-2} (mV)	Reference
P-CoS_2/Ti	1 M KOH	91	This work
CoS_2/Ti	1 M KOH	138	This work
C-CoP-1/12	1 M KOH	173	[2]
Co-P/NF	1 M KOH	43	[3]
p-CoP/CP	1 M KOH	57	[4]
Co_9S_8&$CoS_{1.097}$/RGO	0.5 M H_2SO_4	188	[5]
CoS_2 NP/Al_2O_3 NS	0.5 M H_2SO_4	115	[6]
NCN-1000-5	0.5 M H_2SO_4	90	[7]
Ni_{foam}@Ni-$Ni_{0.2}Mo_{0.8}N$	1 M KOH	15	[8]
NiMnOP/NF	1 M KOH	91	[9]
B-CoP/CNT	0.5 M H2SO4	39	[10]
Mo-CoP	1 M KOH	40	[11]

Table S3. Comparison of UOR performance for P-CoS_2/Ti with other UOR catalysts in recent years.

Electrocatalyst	Electrolyte solution (1 m KOH with)	Potential at 10mA cm^{-2} (V vs.RHE)	Reference
P-CoS_2/Ti	0.3 M urea	1.243	This work
CoS_2/Ti	0.3 M urea	1.336	This work
$Co(OH)_2$&Co+3O(OH)	0.3 M urea	1.536	This work
Co(OH)F/NF	0.7 M urea	1.25	[2]
Ni_3N/NF	0.5 M urea	1.34	[12]
Ni_3N NA/CC	0.33 M urea	1.35	[13]
Ni_2P/CC	0.5 M urea	1.38	[14]
NiCo alloy	0.33 M urea	1.53	[15]
Ni-MOF	0.33 M urea	1.36	[16]
NF/NiMo-Ar	0.5 M urea	1.37	[17]
S-MnO_2-G-NF	0.5 M urea	1.33	[18]
Mn-$Ni(OH)_2$/CFC	0.5 M urea	1.3	[19]

References

1. S. Wei, X. Wang, J. Wang, X. Sun, L. Cui, W. Yang, Y. Zheng and J. Liu, Electrochimica Acta, 2017, 246, 776-782.

2. W. Li, G. Cheng, M. Sun, Z. Wu, G. Liu, D. Su, B. Lan, S. Mai, L. Chen and L. Yu, Nanoscale, 2019, 11, 17084-17092.

3. M. Song, Z. Zhang, Q. Li, W. Jin, Z. Wu, G. Fu and X. Liu, Journal of Materials Chemistry A, 2019, 7, 3697-3703.

4. Y. Zeng, Y. Wang, G. Huang, C. Chen, L. Huang, R. Chen and S. Wang, Chem Commun (Camb), 2018, 54, 1465-1468.

5. X. Sun, H. Huang, C. Wang, Y. Liu, T.-L. Hu and X.-H. Bu, ChemElectroChem, 2018, 5, 3639-3644.

6. L. Fang, Y. Zhang, Y. Guan, H. Zhang, S. Wang and Y. Wang, Journal of Materials Chemistry A, 2017, 5, 2861-2869.

7. H. Jiang, J. Gu, X. Zheng, M. Liu, X. Qiu, L. Wang, W. Li, Z. Chen, X. Ji and J. Li, Energy & Environmental Science, 2019, 12, 322-333.

8. J. Jia, M. Zhai, J. Lv, B. Zhao, H. Du and J. Zhu, ACS Appl Mater Interfaces, 2018, 10, 30400-30408.

9. J. Balamurugan, T. T. Nguyen, V. Aravindan, N. H. Kim and J. H. Lee, Nano Energy, 2020, 69.

10. Z. Chen, E. Cao, H. Wu, P. Yu, Y. Wang, F. Xiao, S. Chen, S. Du, Y. Xie, Y. Wu and Z. Ren, Angew Chem Int Ed Engl, 2019, DOI: 10.1002/anie.201915254.

11. C. Guan, W. Xiao, H. Wu, X. Liu, W. Zang, H. Zhang, J. Ding, Y. P. Feng, S. J. Pennycook and J. Wang, Nano Energy, 2018, 48, 73-80.

12. S. Hu, C. Feng, S. Wang, J. Liu, H. Wu, L. Zhang and J. Zhang, ACS Appl Mater Interfaces, 2019, 11, 13168-13175.

13. Q. Liu, L. Xie, F. Qu, Z. Liu, G. Du, A. M. Asiri and X. Sun, Inorganic Chemistry Frontiers, 2017, 4, 1120-1124.

14. L.-A. Stern, L. Feng, F. Song and X. Hu, Energy & Environmental Science, 2015, 8, 2347-2351.

15. W. Xu, H. Zhang, G. Li and Z. Wu, Sci Rep, 2014, 4, 5863.

16. D. Zhu, C. Guo, J. Liu, L. Wang, Y. Du and S. Z. Qiao, Chem Commun (Camb), 2017, 53, 10906-10909.

17. Z.-Y. Yu, C.-C. Lang, M.-R. Gao, Y. Chen, Q.-Q. Fu, Y. Duan and S.-H. Yu, Energy & Environmental Science, 2018, 11, 1890-1897.

18. C. Xiao, S. Li, X. Zhang and D. R. MacFarlane, Journal of Materials Chemistry A, 2017, 5, 7825-7832.

19. X. Zhang, G. Liu, C. Zhao, G. Wang, Y. Zhang, H. Zhang and H. Zhao, Chem Commun (Camb), 2017, 53, 10711-10714.